BIODIVERSITAS
Volume 27, Number 1, January 2026
Pages: 13

ISSN: 1412-033X
E-ISSN: 2085-4722
https://doi.org/10.13057/biodiv/d270102

Bioactive compounds from *Zanthoxylum acanthopodium* phyllosphere bacteria with antifungal potential against *Candida albicans*

ENNY NUGRAHENI[1,♥], DEBIE RIZQOH[1], LIYA AGUSTIN UMAR[2], SIPRIYADI[3], AZELLA CHIKA FAUZIA[4], SHELLA SHARON[4]

[1]Department of Microbiology and Immunology, Faculty of Medicine and Health Sciences, Universitas Bengkulu. Jl. WR. Supratman, Bengkulu 38371, Bengkulu, Indonesia. Tel.: +62-736-21170, Fax.: +62-736-22105, ♥email: ennynugraheni@unib.ac.id
[2]Department of Medical Biology, Faculty of Medical and Health Science, Universitas Bengkulu. Jl. WR. Supratman, Bengkulu 38371, Bengkulu, Indonesia
[3]Department of Microbiology, Faculty of Mathematics and Natural Sciences, Universitas Bengkulu. Jl. WR. Supratman, Bengkulu 38371, Bengkulu, Indonesia
[4]Department of Medical Education, Faculty of Medicine and Health Sciences, Universitas Bengkulu. Jl. WR. Supratman, Bengkulu 38371, Bengkulu, Indonesia

Manuscript received: 2 July 2025. Revision accepted: 3 January 2026.

Abstract. *Nugraheni E, Rizqoh D, Umar LA, Sipriyadi, Fauzia AC, Sharon S. 2026. Bioactive compounds from* Zanthoxylum acanthopodium *phyllosphere bacteria with antifungal potential against* Candida albicans*. Biodiversitas 27 (1): d270102. https://doi.org/10.13057/biodiv/d270102. Zanthoxylum acanthopodium* (andaliman), an endemic Rutaceae species from Samosir Island, Indonesia, with high economic and medicinal value, harbors phyllosphere bacteria that may produce antifungal metabolites. However, their bioactive compounds remain poorly characterized. This study aimed to identify bioactive compounds from the phyllosphere bacteria of *Z. acanthopodium* and to evaluate their antifungal potential against *Candida albicans*. Phyllosphere bacterial isolates were collected and evaluated against *C. albicans* grown in Potato Dextrose Broth (PDB) using a dilution assay to determine the minimum inhibitory concentration (MIC), and the ethyl acetate extracts were subsequently analyzed by GC-MS to identify constituent compounds. MIC assays showed that the crude extract inhibited *C. albicans* in all isolates at 100% concentration. Molecular identification based on 16S rRNA revealed these isolates as *Brevundimonas* sp. and *Pseudomonas* sp. GC-MS detected phenolic compounds, including isodiospyrin and 1-methyl-ethyl compound. Molecular docking using the *C. albicans* EXO-β-(1,3)-glucanase protein (PDB ID: 1EQP) demonstrated favorable binding energies (ΔG≤0), indicating spontaneous interactions. Isodiospyrin showed the strongest affinity with ΔG –8.56, while the 1-methyl-ethyl compound exhibited the best binding affinity and inhibition constant among the detected compounds. The findings confirm that phyllosphere bacteria of *Z. acanthopodium* exhibit antifungal activity against *C. albicans*. Isodiospyrin and 1-methyl-ethyl compound emerged as promising candidates for further antifungal development. Future studies should validate their efficacy through in vitro and in vivo assays, isolate specific antifungal metabolites, and optimize production for potential therapeutic applications.

Keywords: Antifungal*, Candida albicans*, in vitro, molecular, phyllosphere bacteria

INTRODUCTION

The use of medicinal plants as a source of bioactive compounds has significantly contributed to the discovery of new drugs against microbial infections (Vetvicka et al. 2021). *Zanthoxylum acanthopodium* DC. (andaliman) is a medicinal plant widely used in pharmacology (Adrian et al. 2023; Nurlaeni et al. 2024). Molecular identification revealed two isolates, *Pseudomonas* sp. and *Brevundimonas* sp., as potential sources of bioactive compounds. *Pseudomonas* bacteria can synthesize antibiotics, including mupirocin, gluconic acid, pyrrolnitrin, and 2,4-diacetylphloroglucinol (DAPG) (Baukova et al. 2024). Similarly, *Brevundimonas* sp. isolated from microalgae can produce antimicrobial silver nanoparticles (Rajamanickam et al. 2013).

Zanthoxylum acanthopodium contains secondary metabolites, including antimicrobials and antioxidants, such as flavonoids, alkaloids, terpenoids, and steroids (Hutapea et al. 2024). It works synergistically with bacteria, and this interaction can occur on the leaf surface (phyllosphere) (Nurlaeni et al. 2024). Meanwhile, there are weaknesses in the use of medicinal plants, including chemical composition, seasonality, geographical specificity, and cultivation requirements (Katiyar et al. 2012). Phyllosphere bacteria can produce the same bioactive compounds as host plants and possess antimicrobial compounds that inhibit several pathogenic microbes, including *Escherichia coli*, *Bacillus subtilis*, and *Candida albicans* (Wiederhold 2017; Awidya et al. 2024; Rizqoh et al. 2024a, 2025).

In general, antifungals are used to treat infections caused by *C. albicans*. For example, amphotericin B, echinocandin, azole, and flucytosine are used for invasive candidiasis. Antifungal drugs generally inhibit sterol synthesis in fungal membranes, interact directly with cell membranes, and affect cell wall biosynthesis (Logan et al. 2022). The increase in resistant *Candida* in several countries has become a global health concern, making it difficult for clinicians to provide sensitive treatment (Atriwal et al. 2021; Jawhara 2022). Patients who have received long-term antifungal prophylaxis or antifungal treatment can develop

resistance (Logan et al. 2022). Availability of antifungals follows the number of fungal targets and is similar to that of eukaryotic cells in humans. However, the development of studies to obtain new targets in the genomic era has increased quite sharply in recent times (Brion et al. 2007). A vital cell wall component in *C. albicans* is beta-glucan, which is included in the polysaccharide group called beta-glycosidic, composed of sugar polymer units (Vetvicka et al. 2021).

The rRNA interacts with other RNA molecules to create ribosomes, which play a role in protein synthesis. As the most conserved gene in bacteria, the 16S rRNA gene is particularly useful for identifying the characteristics and distinctions of species. In vitro, molecular and computational methods are used to identify alternative drug repositioning candidates. In-silico drug discovery or Computer-Aided Drug Design (CADD), which is primarily applied in understanding the interaction of chemical compounds with molecular targets, and for use in therapy (Pinzi and Rastelli 2019). In addition, structure-based and ligand-based drug design are efficient virtual screening methods that can be applied with molecular docking (Shaker et al. 2021). Therefore, this research aims to identify the bioactive compound content in the phyllosphere of *Z. acanthopodium* and to analyze its potential as an antifungal candidate against *C. albicans*.

MATERIALS AND METHODS

Reculture of target microbes

Candida albicans was recultured in Potato Dextrose Broth (PDB) and incubated at 37°C for 24 hours. Turbidity was measured using a spectrophotometry (OD = 0.3, concentration 10^6-10^7 cells/mL). The culture was then subjected to an antagonist test.

Antagonist test

Candida albicans culture was mixed with semi-solid Potato Dextrose Agar (PDA) and poured onto solid PDA that had been previously prepared on the plate. The procedure followed the antagonist test method described by Awidya et al. (2024). PDA was placed in the plate's first layer. Following the solidification, a combination of semi-solid Nutrient Agar (NA) and PDB containing *C. albicans* was poured. The bacteria isolated from the phyllosphere appeared at the surface of the hardened layer, and an inhibition zone was observed after 24 hours of incubation. The inhibition zone was categorized following the method by Rizqoh et al. (2024b).

Minimum Inhibitory Concentration (MIC) test

This study used the dilution method to determine MIC on *C. albicans*. The target microbes were recultured for the MIC test in PDB media, then shaken for 24 hours at a speed of 140 RPM at 25°C. The OD of each culture was measured using a spectrophotometer. The incubated isolates were centrifuged at 10,000 RPM for 30 minutes. The supernatant taken was filtered using a 0.22 µm syringe filter and placed into 6 test tubes with different concentrations of 0%, 6.25%, 12.5%, 25%, 50%, and 100%, respectively. All experiments were performed in duplicate (Rizqoh et al. 2024b). A multilevel dilution was performed on the test tube with distilled water. The 0% sample was a negative control, containing NB and 1 mL of target microbes, while the positive control was ketoconazole. Each tube was filled with 1 mL of target microbes. The test culture was incubated for 24 hours, and the OD was measured by spectrophotometry. The MIC was defined as the lowest extract concentration at which the broth remained clear, indicating complete inhibition of microbial growth.

Extraction of bioactive compounds using ethyl acetate

The isolate was cultured in 500 mL of liquid King's B media and incubated on a shaker (100 rpm, 30°C) for 3 days. Subsequently, 150 mL of ethyl acetate was added to the culture and incubated at 40°C for 24 hours, stirred for 20 minutes, and evaporated. The resulting extract was stored at 5°C for further use (Rizqoh et al. 2025).

Gas Chromatography-Mass Spectroscopy (GC-MS) analysis

The crude extract obtained was analyzed using a GC-MS tool to determine the chemical compounds found in phyllosphere bacteria and *Z. acanthopodium* endophytes. *Z. acanthopodium* endophytes were compared with the mass spectrum of known comparative compounds in the database programmed on GC-MS tool (Nikalje and Ramesh 2018).

Molecular detection

The phyllosphere bacteria genome was isolated by separating cultured bacteria (for 24 hours) on King's B media. A 1.5 cc volume of culture was centrifuged for 10 minutes at 10,000 rpm. Following the manufacturer's instructions, genomic DNA was extracted using a bacterial DNA Presto Mini gDNA Bacteria Kit (Geneid).

Two of the best isolates with antibacterial activity were subjected to the 16S rRNA gene amplification. The Polymerase Chain Reaction (PCR) mixture consisted of 12.5 µL PCR buffer GC II, 4 µL dNTPs (2.5 mM/dNTP), 1 µL primer 63 F (`CAGGCCTAACACATGCAAGTC`), 1 µL primer 1387 R (`GGGCGGWGTGTACAAGGC`), 4 µL DNA template, 0.25 µL Taq DNA polymerase (GreenTaq), and 2.25 µL ddH_2O. Amplification was performed in a thermal cycler for 30 cycles under the following conditions: 5 min of predenaturation, 1 min of denaturation at 94°C, 1 min of annealing at 55°C, 1 min of polymerization, and a final extension of 2 min at 72°C. Electrophoresis was used to visualize the 16S rRNA amplicons with a length product of 1300 bp. At Macrogen, Inc., the PCR-amplified gene was subsequently sequenced. Phyllosphere bacteria were identified by analyzing DNA sequences, and homology sequence analysis was used to identify species using the NCBI website Blast-N tool (http://www.ncbi.nlm.nih.gov/).

Molecular docking

Molecular docking of compounds from endophytic bacteria of *Z. acanthopodium* with ligand *C. albicans* was conducted using Lipinski Rule of Five Analysis. In general, this analysis is used to evaluate whether a compound with

antimicrobial activity has chemical and physical properties that can be applied as oral drugs in humans. The potential ligand was examined using the Lipinski Rule of Five criteria by copying the Simplified Molecular Input Line Entry System (SMILES) code from the PubChem site (https://pubchem.ncbi.nlm.nih.gov/) and placing the copy on the Swiss-ADME site (http://www.swissadme.ch/). Evaluation was carried out on compounds with druglike properties (Pinzi and Rastelli 2019).

Preparation of protein and ligand structures

The three-dimensional structure of the ligand was obtained from the PubChem site (https://pubchem.ncbi.nlm.nih.gov/). The search was performed by typing the compound name, chemical formula, or specific ID. The downloaded protein structure was then separated from water molecules and native ligands using BIOVIA Discovery Studio Visualizer software. Subsequently, the protein was optimized using the AutoDock application to add polar hydrogen atoms and saved in the pdbqt format (Prieto-Martínez et al. 2018). The three-dimensional structures of ligands positively identified in the phytochemical test were downloaded from the NCBI PubChem Compounds website, database (www.pubchem.ncbi.nlm.nih.gov/), and ChemSpider (http://www.Chemspider.com/) in sdf format. Optimization was performed by changing the initial (.sdf) into a file format that can be read in the AutoDock docking application (.pdbqt). The receptor and ligand files used in the in silico test were saved in the pdbqt format in the same folder containing all data related to the materials and docking result files.

Determining protein docking site

The docking site was located at the binding position for the ligand during the docking process. A grid box was created in the AutoDock application to determine the docking site. Data related to the dimensions and coordinates of the grid box were stored in the format "grid.txt". This dimension and coordinate data were then used in molecular docking through the AutoDock application.

Molecular docking method

Validation was conducted after successfully identifying docking position. This was achieved by docking between the protein and the native ligand previously separated in the preparation process, also called redocking. The parameter often used is RMSD (Root Mean Square Deviation). The method is considered valid when RMSD value is ≤2, suggesting the feasibility of docking. A test compound with the target protein in the same grid box area was carried out using the AutoDock application. The higher the deviation, the greater the error in predicting ligand interactions with protein (Pratama et al. 2021).

Data analysis

The results were analyzed using several parameters, namely Gibbs free energy (ΔG) obtained from docking of each ligand to the protein receptor, ligand-protein complexes, and residue-ligand interactions visualized with BIOVIA Discovery Studio Visualizer.

RESULTS AND DISCUSSION

Antagonist test of phyllosphere bacteria against *Candida albicans*

A total of 64 phyllosphere bacterial isolates were screened for their antagonist activity against *C. albicans*. As shown in Table 1, four isolated strains demonstrated significant activity as indicated by the presence of an inhibition zone around the phyllosphere bacteria spotted on semi-solid media (Figure 1). The inhibition zone produced can be classified as weak or moderate. The diameter of the inhibition zone activity in AF49, AF50, AF53, and AF56 was 5.2 mm, 5.3 mm, 2.5 mm, and 4.4 mm, in the moderate, moderate, weak, and weak categories, respectively.

MIC of phyllophere bacteria to *Candida albicans*

Based on the results of the MIC test, a concentration of 100% had inhibitory power in all three phyllosphere isolates, 50% and 25% had inhibitory power only in isolates AF 49 and AF 50, while 12.5% and 6.25% did not show any inhibitory power in all three isolates. The control media appeared clear, indicating no bacterial growth, and the positive control (+) also appeared clear, consistent with ketoconazole's antimicrobial activity (Table 1). The observation results were then confirmed using spectrophotometry, as shown in Table 2.

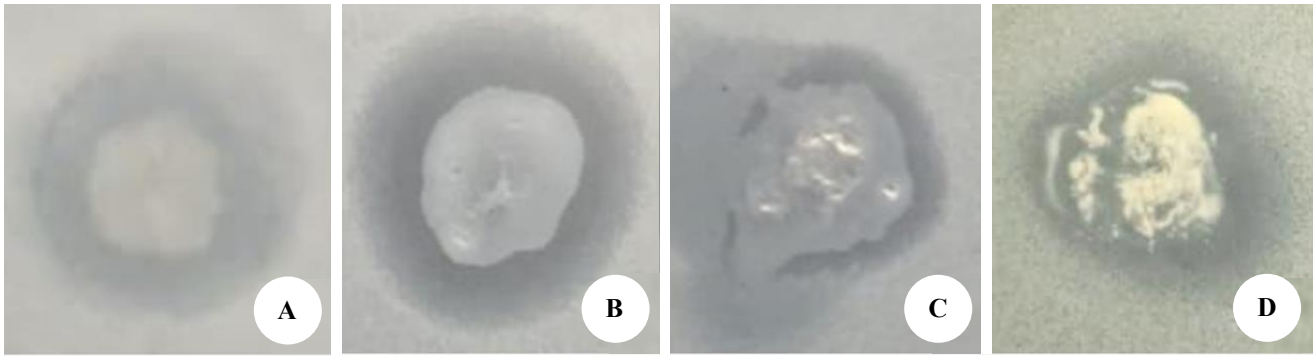

Figure 1. Inhibition zone from antagonist test of *Zanthoxylum acanthopodium* phyllosphere bacterial isolates: A. AF 49, B. AF 50, C. AF 53, and D. AF 56 against *Candida albicans*

Extraction of *Z. acanthopodium* phyllosphere bacteria

The extraction process for *Z. acanthopodium* phyllosphere bacteria was performed on isolates AF49, AF50, and AF56. During the extraction process, the stock culture isolates from the previous glycerol media were rejuvenated into working cultures by streaking onto Nutrient Agar (NA) and incubating for 24 hours. After growth, each was cultured in 25 mL of Nutrient Broth (NB) and incubated for 24 hours. The culture isolates were multiplied by transferring them to 250 mL of NB media and incubating for 3 × 24 hours to obtain secondary metabolites in the stationary phase. The new culture was added with 250 mL of ethyl acetate solvent, and mixed for 24 hours in an incubator shaker. The bacteria concentrate bound by ethyl acetate solvent compound was separated using a separating funnel. The concentrate was then evaporated using a rotary evaporator to obtain a crude extract. Table 3 presents the extraction results for the three *Z. acanthopodium* phyllosphere bacterial isolates.

Bioactive compounds of *Z. acanthopodium* phyllosphere bacteria

Bioactive compounds in *Z. acanthopodium* phyllosphere bacteria extract were analyzed using the GC-MS method. The reading results were in the form of chromatograms and spectrum graphs for extracts numbers 49 (Figure 2), 50 (Figure 3), and 56 (Figure 4). The chromatogram was interpreted by reading the peaks of each chromatogram, showing more than 20 bioactive compounds (Table 4, Table 5, Table 6).

Molecular identification of *Z. acanthopodium* phyllosphere bacteria

The established base sequences of the 16S rRNA coding gene serve to identify bacteria species by using data from the gene bank that incorporates previously recognized similar organisms. Analysis of the gene bank data showed that AF49 and AF50 had the highest similarity to *Brevundimonas* sp. (99.10%), and *Pseudomonas* sp. (80.58%).

Molecular docking

Lipinski rule of five criteria test on SwissADME

Phytochemical data for the 70% ethanol extract were analyzed at the Forensic Laboratory of the Criminal Investigation Department of the Indonesian National Police using GC-MS. The results showed 15 compounds, with two from the flavonoid group and three from the alkaloid group. The screening was conducted to identify active compounds with antifungal activity against *C. albicans*. To proceed to the molecular docking stage, compounds must meet the druglikeness properties test with the Lipinski rule of five criteria. Based on the test results, isodiosipyrine and methylethyl-monoterpenoid met the criteria, suggesting the compounds can be further evaluated in the docking stage for drug development studies.

Ligand and receptor downloading

In this study, the ligand consisted of phenolic compounds identified through phytochemical screening of *Z. acanthopodium* phyllosphere bacterial extracts. The ligand selected for docking was based on GC-MS results or was available on the PubChem site (https://pubchem.ncbi.nlm.nih.gov/). The receptor protein, *C. albicans* Beta-Glucan, was downloaded through the PDB site (www.rcsb.org) by entering the name or specific ID of *C. albicans* EXO-B-(1.3)-Beta-glucanase protein (PDB ID 1EQP) in the search column (Figure 5). The receptor was selected based on X-ray diffraction resolution, macromolecular validation, and molecular size. The macromolecules used should have a maximum resolution of 2 Å. The lower the resolution value, the better the docking results. In the validation section, several parameters describe the quality of the macromolecules. The further to the right of the "slider" graph (blue), the better the quality of the macromolecules used. The size of the molecule used should be above 100 kDa because the quality of the resulting interaction will be higher (Pinzi and Rastelli 2019).

Table 1. Result of MIC test phyllophere bacteria

Concentration of phyllosphere supernatant	AF 49	AF 50	AF 56
100%	-	-	-
50%	-	-	+
25%	-	-	+
12.5%	+	+	+
6.25%	+	+	+
Control M	-	-	-
Control (+)	-	-	-
Control (-)	+	+	+

Note: +: Positive: Cloudy (bacterial growth), -: Negative: Clear (no bacterial growth). Control M: Media, Control -: NB contains target microbes, Control +: NB contains target microbes and antibiotics

Table 2. Results of optical density MIC of phyllosphere bacterial

Tube number	Concentration	AF 49	AF 50	AF 56
1	100%	0.3566	0.3504	0.2946
2	50%	0.4386	0.3789	0.4004
3	25%	0.4221	0.3747	0.4061
4	12.5%	0.5046	0.4845	0.4892
5	6.25%	0.5311	0.5299	0.4616
6	Control M		0.0259	
7	Control (+)		0.0470	
8	Control (-)		0.6437	

Note: Control M: Media, Control -: NB contains target microbes, Control +: NB contains target microbes and antibiotics

Table 3. Results of the extraction of *Zanthoxylum acanthopodium* phyllosphere bacteria isolates

Isolate	Extract volume
AF 49	2.3 mL
AF 50	1.5 mL
AF 56	0.25 mL

Table 4. Identification of bioactive compounds from *Zanthoxylum acanthopodium* phyllosphere bacteria extract-49

Compound name	RT (min)	Molecular formula	Compound composition (%)	Classification
Heptadecane	9.963	$C_{17}H_{36}$	0.20	Alkanes
Heptane, 2,6-dimethyl-	10.004	C_9H_{20}	0.23	Aliphatics hydrocarbon
3-methyl-3-cyclohexen-1-ol	10.086	$C_7H_{12}O$	0.57	Secondary alcohol
Octadecane	10.699	$C_{18}H_{38}$	0.36	Aliphatics hydrocarbon
4-Decene, 8-methyl- (E)-	11.027	$C_{11}H_{22}$	0.39	N/a
1-Pentadecene	11.402	$C_{15}H_{30}$	0.38	Hydrocarbon
Pentadecanoic acid, 14-methyl-, methyl ester	11.584	$C_{17}H_{34}O_2$	9.43	Fatty acid methyl ester
2-Hydroxy-3,5,5-trimethyl-cyclohex-2-enone	11.696	$C_9H_{14}O_2$	0.44	Alicyclic ketone
Pyrrolo(1,2-a) pyrazine-1,4-dione,hexahydro-3-(2-methylpropyl)	11.824	$C_{11}H_{18}N_2O_2$	1.00	Organonitrogen
2-Decene, 3-methyl-, (z)-	11.898	$C_{11}H_{22}$	0.54	Organic
1-Pentadecene	12.072	$C_{15}H_{30}$	0.39	Hydrocarbon
9-Octadecenoic acid, Oleic acid	12.624	$C_{18}H_{34}O_2$	0.27	Fatty acid
Oleic acid methyl ester	12.738	$C_{19}H_{36}O_2$	12.54	Fatty acid
Methyl stearate, Octadecanoic acid, Methyl ester	12.892	$C_{19}H_{38}O_2$	1.78	Fatty acid
9-Octadecenoic acid, Oleic acid	13.091	$C_{18}H_{34}O_2$	0.33	Fatty acid
17,21-Dimethylheptatriacontane	13.383	$C_{39}H_{80}$	1.61	Hydrocarbon
2-hydroxy-1-(hydroxymethyl) ethyl ester, 2-Monoolein	13.503	$C_{21}H_{40}O_4$	0.14	Glyceride
4,4-Dideutero heptadecanal	13.693	$C_{17}H_{32}D_{20}$	0.89	Fatty aldehyde
9-Octadecenoic acid, Oleic acid	13.846	$C_{18}H_{34}O_2$	0.21	Fatty acid
2,3-dihydroxypropyl ester, Olein	14.153	$C_{21}H_{40}O_4$	0.56	Fatty acid
Oleic acid	15.265	$C_{18}H_{34}O_2$	0.58	Fatty acid
[1,2'-Binaphthalene]-5,5',8,8'-tet rone, 1',4-dihydroxy-2,3' dimethyl, Isodiospyrin	25.335	$C_{22}H_{14}O_6$	26.62	Quinones (naphthoquinones)
21H-B iline-3-acetic acid, 17-ethyl-1,2, 3,19,23,24 hexahydro-2,2,7,8,12,13,18,21,24-nonamethyl-1 ,19-dioxo-, methyl ester,	25.443	$C_{32}H_{40}N_4O_4$	7.33	Peptide
[1,2'Binaphthalene]-5,5',8,8'-tetrone, 1',4-dihydroxy-2,3'-dimethyl -, (-)-	25.550	$C_{22}H_{14}O_6$	2.70	Quinones (naphthoquinones)
Tetradecanal	25.645	$C_{14}H_{28}O$	2.32	Aldehydes
Tetradecanal	25.681	$C_{14}H_{28}O$	1.17	Aldehydes
Tetradecanal	25.777	$C_{14}H_{28}O$	2.22	Aldehydes
9-Eicosyne	25.918	$C_{14}H_{28}O$	4.31	Aldehydes
Cyclohexaneethanol, 4-methyl-.beta .-methylene-, trans-	26.018	$C_{10}H_{18}O$	2.60	Volatile

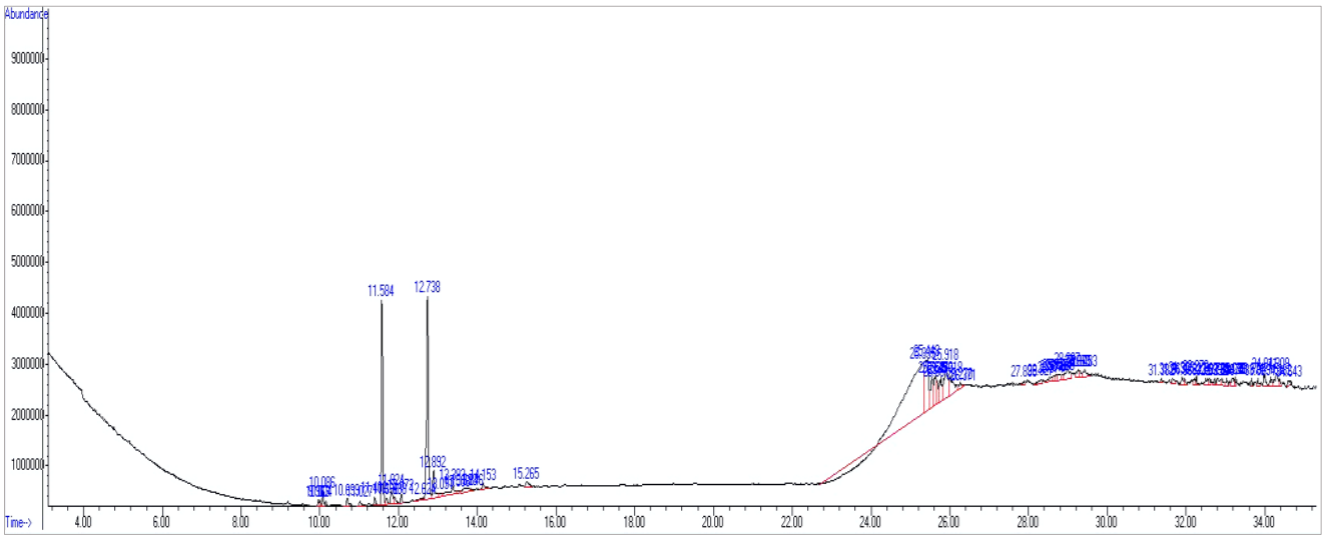

Figure 2. Gas Chromatography-Mass Spectrometry (GC-MS) chromatogram of bioactive compounds from *Zanthoxylum acanthopodium* phyllosphere bacteria extract-49

Table 5. Identification of bioactive compounds from *Zanthoxylum acanthopodium* phyllosphere bacteria isolate 50

Compound name	RT (min)	Molecular formula	Compound composition (%)	Classification
2-Furanmethanol (CAS), Furfuryl alcohol	10.081	$C_5H_6O_2$	0.67	Aromatic alcohol
2-Methylene-cyclopentanol	11.822	$C_6H_{10}O$	0.33	Cyclic alcohol
9-Octadecenoic acid (Z)- (CAS), Oleic acid	12.358	$C_{18}H_{34}O_2$	0.11	Fatty acid
9-Octadecenoic acid (Z)- (CAS), Oleic acid	12.708	$C_{18}H_{34}O_2$	0.13	Fatty acid
Aspidospermidin-17-ol, 1-acetyl-19,21-epoxy-15,16-dimethoxy-	13.133	$C_{23}H_{30}N_2O_5$	0.23	Kopsane alkaloid
9-Octadecenoic acid (Z)- (CAS), Oleic acid	13.243	$C_{18}H_{34}O_2$	0.08	Fatty acid
8-Heptadecyne, 1-bromo-	13.374	$C_{17}H_{31}Br$	0.03	Alkyne
9-Octadecenoic acid (Z)- (CAS), Oleic acid	23.095	$C_{18}H_{34}O_2$	0.08	Fatty acid
13-Tetradecenal	23.406	$C_{14}H_{26}O$	0.05	Fatty aldehyde
Octadecanal, Stearaldehyde	24.544	$C_{18}H_{36}O$	9.22	Fatty aldehyde
9-Octadecenoic acid (Z)- (CAS), Oleic acid	24.907	$C_{18}H_{34}O_2$	8.63	Fatty acid
2,5-Cyclohexadiene-1,4-dione, 3-hydroxy-2-methyl-5-(1-methylethyl)-	25.108	$C_{10}H_{12}O_3$	7.39	Mono Terpenoid
2,5-Cyclohexadiene-1,4-dione, 3-hydroxy-2-methyl-5-(1-methylethyl)-	25.460	$C_{10}H_{12}O_3$	14.63	Mono Terpenoid
Ethanol, 2-(tetradecyloxy)-	25.574	$C_{16}H_{34}O_2$	5.49	Fatty alcohol
(cis)-2-nonadecene	25.723	$C_{19}H_{38}$	6.37	Alkane hydrocarbon
9-Octadecenoic acid (Z)- (CAS), Oleic acid	25.846	$C_{18}H_{34}O_2$	4.18	Fatty acid
(Z,Z)-4-Ethyl-3-methyl-5-(5-(3,4-dimethyl-1H-pyrrolyl-2-methylen)-4-(2-caboxyethyl)-3-methyl-5H-pyrrolyl-2-methylen)-3-pyrrolin-2-on	25.887	$C_{23}H_{27}N_3O_3$	6.08	Aromatic
9-Octadecenoic acid (Z)-, tetradecyl ester, Oleic acid, tetradecyl ester	26.047	$C_{32}H_{62}O_2$	4.34	Unsaturated ester
9-Octadecenoic acid (Z)- (CAS), Oleic acid	26.175	$C_{18}H_{34}O_2$	2.60	Fatty acid
Cyclopentane, 1,1'-[4-(3-cyclopentylpropyl)-1,7-heptanediyl]bis-	26.312	$C_{25}H_{46}$	5.72	Hydrocarbon
[1,2'-Binaphthalene]-5,5',8,8'-tetrone, 1',4-dihydroxy-2,3'-dimethyl	26.429	$C_{22}H_{14}O_6$	5.22	Phenols quinone/hydroquinone
Cyclopentane, 1,1'-[4-(3-cyclopentylpropyl)-1,7-heptanediyl]bis-	26.660	$C_{25}H_{46}$	4.01	Hydrocarbon
9-Octadecenoic acid (Z)- (CAS), Oleic acid	26.719	$C_{18}H_{34}O_2$	1.32	Fatty acid
(12z)-7.beta.-acetoxy-6.beta.,8-bis(trimethylsilanyloxy)-labda-12,14-dien-11-one	26.839	$C_{28}H_{50}O_5Si_2$	4.68	Organosilicon
Dipalmitoylphosphatidylethanolamin	26.931	$C_{37}H_{74}NO_8P$	5.00	Phospholipid

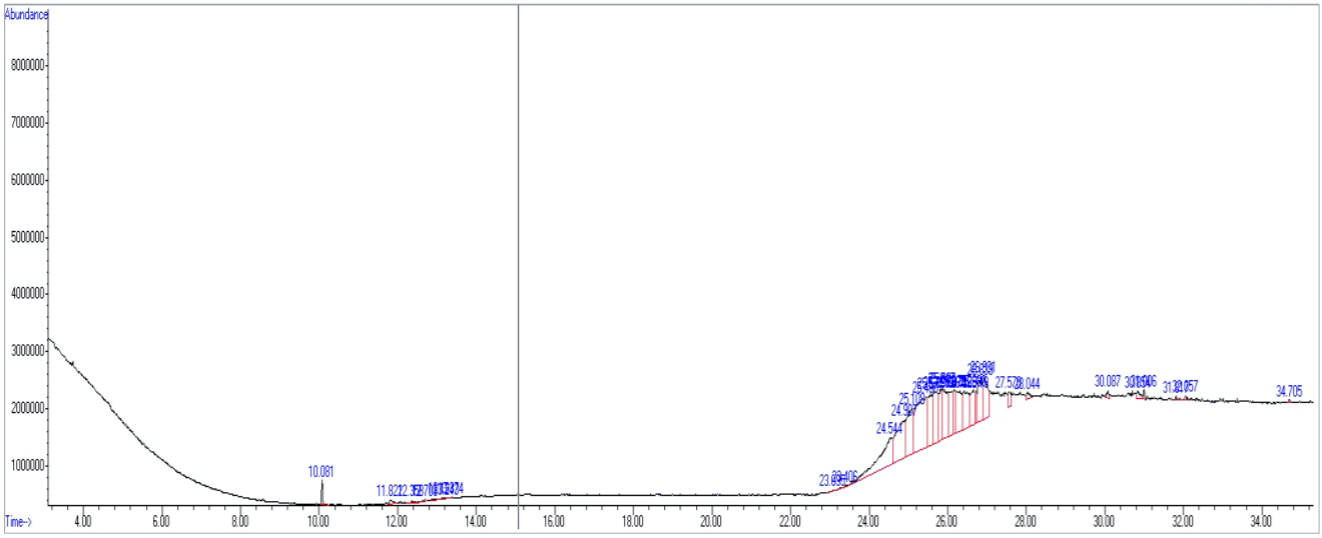

Figure 3. Gas Chromatography-Mass Spectrometry (GC-MS) chromatogram of bioactive compounds from *Zanthoxylum acanthopodium* phyllosphere bacteria isolate-50

Table 6. Identified of bioactive compounds from *Zanthoxylum acanthopodium* phyllosphere bacteria isolate-56

Compound name	RT (min)	Molecular formula	Compound composition (%)	Classification
HEXANOL-4-D2	3.729	$C_6H_{12}D_2O$	0.59	Alcohol
1,3-Oxathiol-1-ium, 4-hydroxy-2 [(1-methyl ethyl) thio]-5-(trifluoroacetyl)-, hydroxide, inner salt (CAS)	5.107	$C_8H_5F_3O_3S_2$	0.18	Aromatic
2-Furanmethanol (CAS), Furfuryl alcohol	10.078	$C_5H_6O_2$	0.48	Aromatic alcohol
1-Tetradecanol (CAS), Alfol	11.016	$C_{14}H_{30}O$	0.20	Fatty alcohol
8-Hexadecenal, 14-methyl-,	11.682	$C_{17}H_{32}O$	0.19	Fatty aldehyde
Pyrrolo[1,2-a]pyrazine-1,4-dione	11.809	$C_{11}H_{18}N_2O_2$	0.49	Alpha-amino acid
3-Undecene	11.885	$C_{11}H_{22}$	0.24	Hydrocarbon
13-Tetradecenal	12.706	$C_{14}H_{26}O$	0.14	Fatty aldehyde
Z,Z-6,13-Octadecadien-1-ol acetate	13.130	$C_{20}H_{36}O_2$	0.33	Fatty alcohol
12,13-epoxy-9,15-octadec-diene	13.236	$C_{18}H_{32}O$	0.06	Polyunsaturated fatty acid
4,4-dideutero heptadecanal	15.243	$C_{17}H_{322}D_2O$	0.28	Aromatic
12,13-epoxy-9,15-octadec-diene	23.154	$C_{18}H_{32}O$	0.13	Polyunsaturated fatty acid
9-Octadecenoic acid (Z)- (CAS), Oleic acid	23.893	$C_{18}H_{34}O_2$	1.08	Fatty acid
2-Nonenal, 8-oxo-	23.947	$C_9H_{14}O_2$	0.31	Fatty aldehyde
Octadecanal, Stearaldehyde	24.149	$C_{18}H_{36}O$	1.58	Fatty aldehyde
2-(4-hydroxybutyl)-2- nitrocyclodecanone	24.225	$C_{16}H_{29}NO_4$	0.98	Cyclic ketone
Hexadecanal	24.455	$C_{16}H_{32}O$	4.60	Fatty aldehyde
Hexadecanal	24.693	$C_{16}H_{32}O$	6.15	Fatty aldehyde
2,5-Cyclohexadiene-1,4-dione, 3-hydroxy-2-methyl-5-(1-methylethyl)-	25.375	$C_{10}H_{12}O_3$	31.56	Mono Terpenoid
[1,2'-Binaphthalene]-5,5',8,8'-tetrone, 1',4-dihydroxy-2,3'-dimethyl	25.450	$C_{22}H_{14}O_6$	2.95	Phenols quinone/hydroquinone
Ethanol, 2-(tetradecyloxy)-	25.502	$C_{16}H_{34}O_2$	3.32	Fatty alcohol
Ethanol, 2-(tetradecyloxy)-	25.571	$C_{16}H_{34}O_2$	2.34	Fatty alcohol
Ethanol, 2-(tetradecyloxy)-	25.626	$C_{16}H_{34}O_2$	3.21	Fatty alcohol
HAHNFETT	25.719	N/A	5.65	N/a
(Z,Z)-4-Ethyl-3-methyl-5-(5-(3,4-dimethyl-1H-pyrrolyl-2-methylen)-4-(2-caboxyethyl)-3-methyl-5H-pyrrolyl-2-methylen)-3-pyrrolin-2-on	25.781	$C_{23}H_{27}N_3O_3$	2.47	Aromatic
2,5-Cyclohexadiene-1,4-dione, 3-hydroxy-2-methyl-5-(1-methylethyl)-	25.833	$C_{10}H_{12}O_3$	5.40	Mono Terpenoid
Cyclotetracosane	25.945	$C_{24}H_{48}$	3.99	Aliphatic hydrocarbon

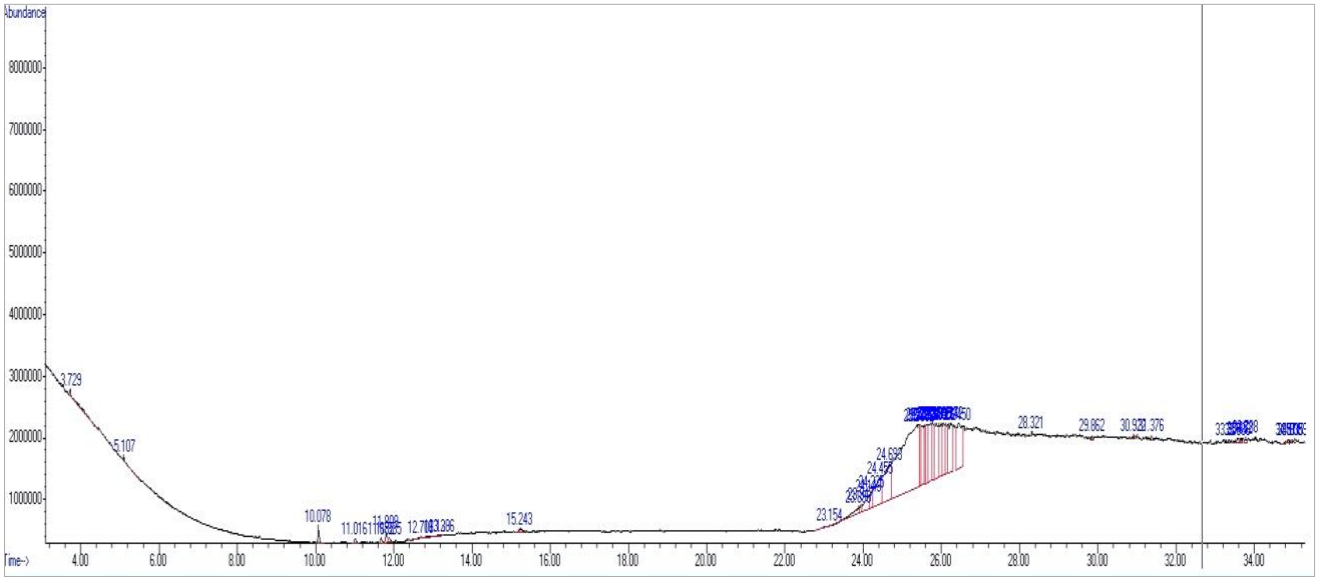

Figure 4. Gas Chromatography-Mass Spectrometry (GC-MS) chromatogram of bioactive compounds from *Zanthoxylum acanthopodium* phyllosphere bacteria extract 56

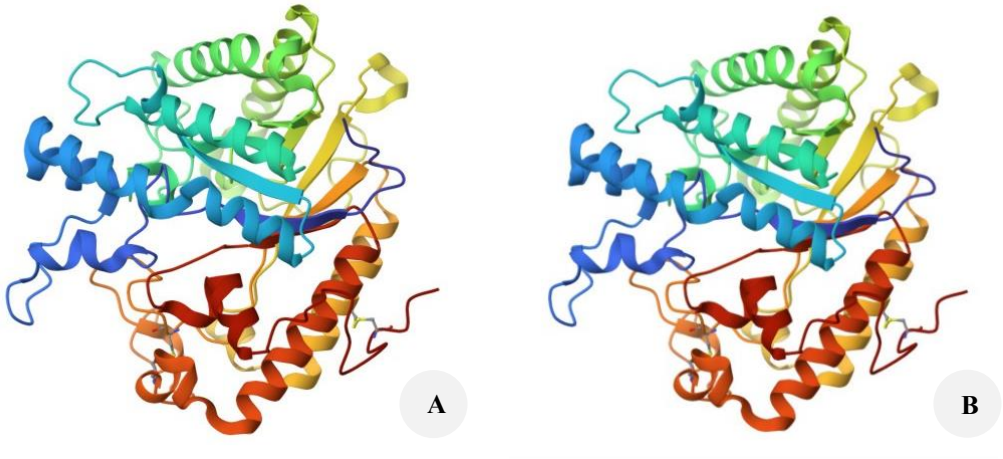

Figure 5. Structure of receptor downloading on PDB site. A. 1EQP. Exo-b-(1,3)-glucanase from *Candida albicans*, B. 1CZ1 exo-b(1,3)-glucanase from *Candida albicans*

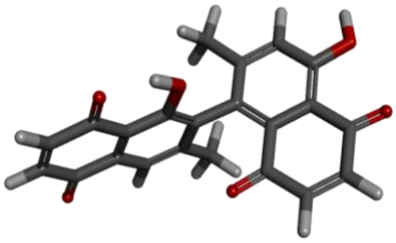

Figure 6. Isodiospyrin 3D ligand structure

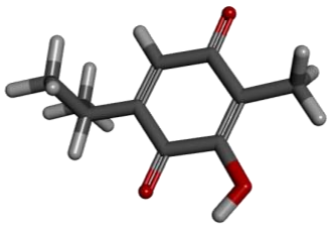

Figure 7. 1-Methylethyl 3D ligand structure

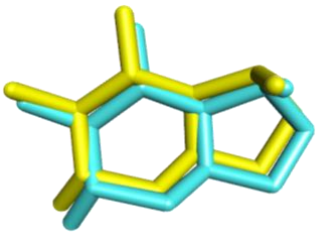

Figure 8. Structure of overlapping position between the position of the native ligand before re-docking (yellow) and the position of the native ligand after re-docking (blue)

Validation of the docking method

Validation of the docking method was carried out by re-docking the native ligand in the active site of the receptor. The process started by separating the protein (PDB ID: 5JJR) from the native ligand. Redocking of the native ligand was run 10 times to determine the position with the best RMSD value. The docking method is considered valid when RMSD value is ≤2 Å. Based on the results, the lowest RMSD value of the native ligand SAH was 1.10 Å with a binding free energy of -9.53 kcal/mol. For the 68E ligand, RMSD value of 1.45 Å and a binding free energy of -9.70 kcal/mol were recorded. These values confirm the method's validity, as the ligand positions after docking closely overlapped with original configurations in the 3D structure (Figure 6 and 7), with native ligand positions before (yellow) and after (blue) re-docking visually aligned (Figure 8).

Redocking of the native ligand was performed on the active site of the receptor to validate docking method. The process started by separating the protein (PDB ID 1EQC) from the native ligand. Redocking of the native ligand was performed 10 times to determine the position with the best RMSD value. The docking method is considered valid when RMSD value is ≤2 Å. The results showed that the lowest RMSD value of the native ligand SAH was 0.43 Å with a binding free energy of -8.57 kcal/mol. Visualization of docking method using Biovia Discovery Studio shows the overlapping position between the position of the native ligand before re-docking (yellow) and the position of the native ligand after re-docking (Figure 8).

Docking

Molecular docking process using AutodockTools software produces files in .pdbqt format; hence, it is necessary to use the additional application Biovia Discovery Studio in 2D and 3D. Visualization of interactions in 2D is shown in Table 7 and Table 8 is presented visualization amino acid interactions and Figure 9 is presented visualization amino acid ligan 2D interactions display amino acid.

Each color in 2D indicates the type of interaction formed. In the re-docking process, the native ligand CTS produced 13 amino acid residues and forms 5 hydrogen bonds found in the glutamate sequence 27 and 292 (GLU27, GLU292), asparagine 191 (ASN191), histidine 135 (HIS135), and

tyrosine sequence 29 (TYR29). Visualization of the protein with the isodiospyrin ligand produced 16 amino acid residues, with 3 having hydrogen bonds. The hydrogen bonds formed are found in the glutamate 192 (GLU192) and tyrosine sequence 29 (TYR29). Protein interaction with 2,5-cyclohexadiene-1,4-dione ligand, 3-hydroxy-2-methyl-5-(1-methylethyl) formed 13 amino acid residues. Hydrogen bonds were formed at the 135th amino acid histidine (HIS135), the 191st amino acid asparagine (ASN191), and the 29th amino acid tyrosine (TYR29).

Binding affinity (Gibbs free energy/ΔG) is a crucial metric in molecular docking that predicts a compound's capacity to influence a target protein. The stability of the complex between ligand and protein can be predicted by the Gibbs free energy (ΔG), which is negative when molecular interactions result in a stable complex. Stronger and more stable bonds are created when the test compound and the target protein have lower binding energy values (Zhang et al. 2022). As shown in Table 9, the energy values of the two test ligands, namely Isodiospyrin and 1-methylethy, were -8.56 and -5.84, while that of CTS (native ligand) was -8.56 kcal/mol. The two compounds extracted show negative docking score values, suggesting feasible interaction with *C. albicans* Exo-B-(1.3)-glucanase protein active site. The test ligand Gibbs energy value is similar to that of the native, suggesting the molecules Isodiospyrin bind to the target protein with similar strength as the original ligand binds (receptor). A lower (more negative) docking score reflects a greater tendency that the ligand forms a stable complex with the target protein, enhancing the potential as a candidate for further antifungal drug development (Zhang et al. 2022).

Discussion

Candida is a fungus that causes opportunistic infections that affect the vagina, mouth, penis, and other parts of the body. The results show (Table 1) that *Z. acanthopodium* phyllosphere bacteria can inhibit *C. albicans.* Phyllosphere bacteria produce bioactive compounds that inhibit certain pathogenic microbes (Rizqoh et al. 2025). A previous study confirmed that phyllosphere bacteria from *Plumeria acuminata* showed strong potential to inhibit *C. albicans* (Awidya et al. 2024). Phyllosphere bacteria from *Z. acanthopodium* also inhibited the growth of *B. subtilis* and *S. aureus*. *Z. acanthopodium*, known as endemic Samosir Island vegetation a member Rutacea family with high economy value, antimicrobial benefits that can be used as medicine, and natural antioxidant. *Z. acanthopodium* grows lushly in a subtropical climate in the Himalayan mountains (Rizqoh et al. 2024b).

In this study, the phyllosphere bacteria of *Z. acanthopodium* exhibited antifungal activity, as evidenced by the formation of an inhibitory zone around the isolate when injected into the test medium. These results are consistent with studies stating that the endophytic fungi of *Z. acanthopodium* can inhibit fungal growth. Furthermore, Kintamani et al. (2023) demonstrated that *Z. acanthopodium* fruit extract demonstrated bactericidal effect against *Bacillus* sp. The extract exhibits range of biological properties, including larvicidal, anti-inflammatory, antioxidant, analgesic, antibacterial, and antifungal activities. Bioactive compounds in andaliman, such as essential oils, alkaloids, flavonoids, saponins, and tannins, exhibit antimicrobial activity that can reduce bacterial colony counts. According to Pelczar and Chan (2008), antimicrobial compounds generally function by damaging cell walls, changing membrane permeability, disrupting protein synthesis, and inhibiting enzyme activity.

Table 7. Visualization of test ligand interaction with EXO-B-(1,3)-glucanase protein receptor in 2 dimensions

Ligand	2D visualization of ligand-receptor interactions
Native ligand CTS (control)	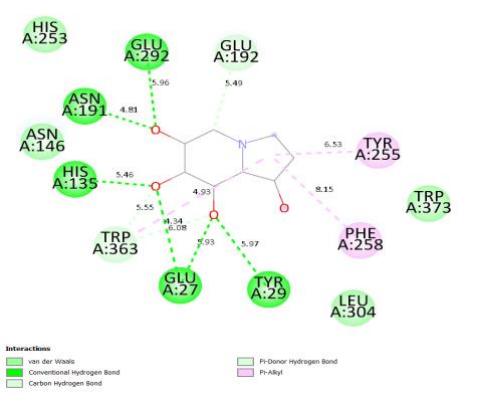
Isodiospyrin	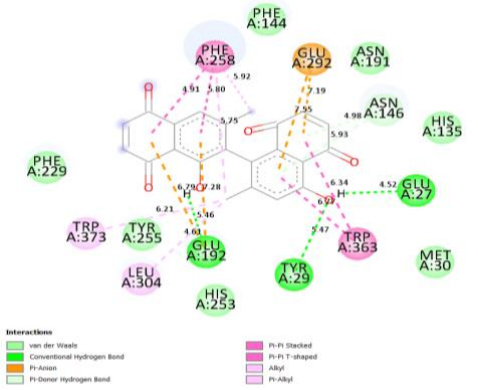
2,5-cyclohexadiene-1,4-dione, 3-hydroxy-2-methyl-5-(1-methylethyl)	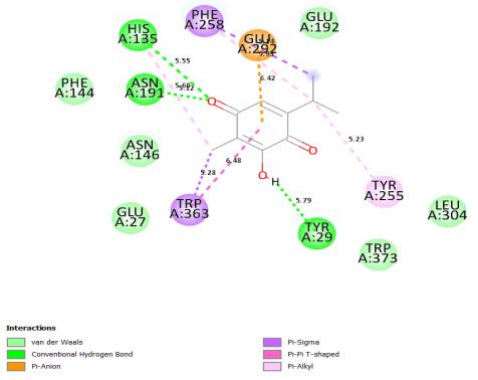

Note: Interaction variation (Biovia Discoveru Studio Visualizer)

Table 9. Docking results of test ligands with EXO-B-(1,3)-glucanase protein receptor at the native ligand CTS binding site

Macromolecule	Ligand	Binding affinity ΔG (kkal/mol)	Inhibit constanta(uM)	Hydrogen bond
EXO-B-(1,3)-glucanase (PDB ID 1EQC)	CTS (Control)	-8.56	526.82	GLU27, GLU292, ASN191, HIS135, TYR29
	Isodiospyrin	-8.56	533.76	GLU27, GLU192, TYR29
	2,5-cyclohexadiene-1,4-dione, 3-hydroxy-2-methyl-5-(1-methylethyl)	-5.84	52.37	HIS135, ASN191, TYR29

Table 8. Visualization of test ligand interaction with EXO-B-(1,3)-glucanase protein receptor in 3 dimensions

Ligand	2D visualization of ligand-receptor interactions
Native ligand CTS (control)	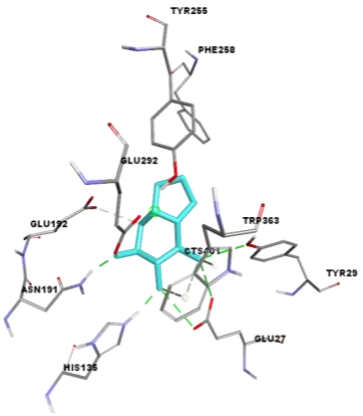
Isodiospyrin	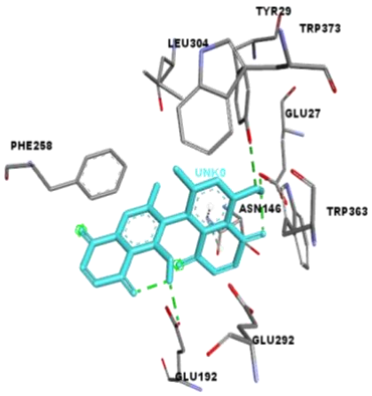
2,5-cyclohexadiene-1,4-dione, 3-hydroxy-2-methyl-5-(1-methylethyl)	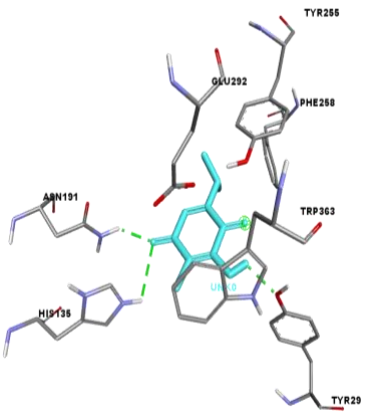

Note: Visualization of native ligand and test ligand interactions in 3D shows the position of the ligand during interaction and the amino acid residues of the receptor (gray). The test ligand is shown in blue to distinguish ligands with formed bond interactions

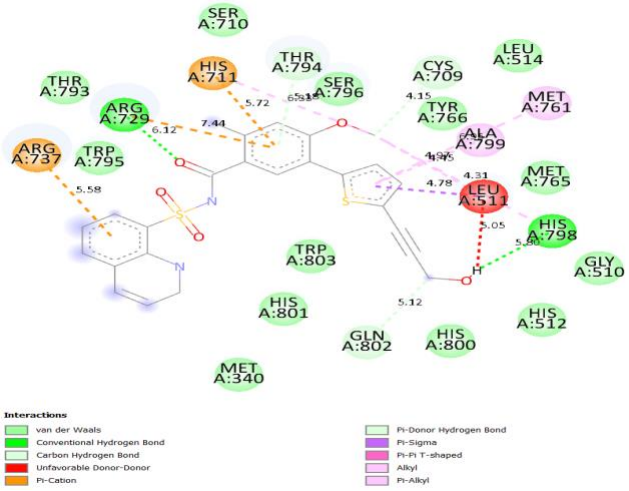

Figure 9. 2D interactions display amino acid residues and ligand-receptor interactions formed

MIC test of phyllosphere isolates against *C. albicans* with AF49 and AF50 codes at concentrations of 6.25% and 12.5% showed turbidity in the test tube, suggesting microbial growth. Meanwhile, at concentrations of 25%-100%, the test tube remained clear, indicating no growth. The visual and spectrophotometric observations showed that the 100% concentration produced the most significant results, visually appearing clear. The spectrophotometry results also showed that 100% had the lowest OD compared to other concentrations. MIC test against *C. albicans* demonstrated effectiveness at a concentration of 100%, but at 50%, turbidity was observed in 1 of the 3 test tubes.

Bioactive compounds in andaliman, such as alkaloids, flavonoids, saponins, and tannins, have antimicrobial activity. The bioactive compounds have different mechanisms for inhibiting microbial growth. The mechanism of flavonoids starts with the formation of a receptor-glycoside complex through hydrogen bonds that degrade after passing through the cell membrane. Penetration of the compound into the cell membrane causes coagulation of protein and cell membrane, thereby inhibiting the process of cell wall formation and lysis (Soeka et al. 2007). Saponin compounds work by increasing permeability and reducing surface tension of the cell wall, causing leakage of intracellular nutrients, which leads to death (Yu et al. 2022). Antimicrobial effect of tannins is through reactions with cell membranes, enzyme inactivation, and destruction or inactivation of genetic material function (Huang et al.

2024). According to this study, the phyllosphere bacteria species detected in Andaliman include *Pseudomonas* sp. and *Brevundimonas* sp. This result is similar to previous studies on other plants, such as apple, whose phyllosphere is mainly composed of taxa including *Pseudomonas* and Enterobacteriaceae (Steven et al. 2018). *Pseudomonas* is the most prevalent, according to several studies (Johnston-Monje and Raizada 2021).

Azoles remain the primary treatment for infections caused by *C. albicans*, with fluconazole being the most commonly prescribed. This group of antifungals works by inhibiting 14-α-sterol demethylase encoded by the ERG11 gene, an enzyme that plays a crucial role in the biosynthesis of the fungal-specific membrane sterol ergosterol. Given that some *C. albicans* species show intrinsic resistance to azoles, the use is probably a contributing factor to the higher incidence of infections. In addition, many studies have documented the ability of *Candida* to develop high-level resistance to azole antifungals (Bras et al. 2024).

The complex and dynamic structure of *C. albicans* cell wall is composed of an exterior layer or matrix made up primarily of mannose-glycosylated protein and a core structure of beta-(1,3)-glucan covalently bonded to beta-(1-6)-glucan and chitin. The interface between the pathogen and the host is the fungal cell wall surface, which is glycosylated by mannose. Numerous Pathogen Recognition Receptors (PRRs), such as TLR receptors and C-type lectins, can sense the highly conserved Pathogen-Associated Molecular Patterns (PAMPs) on the surface of the fungal cell wall, making it a useful therapeutic target. PRRs play a role in the synthesis of proinflammatory cytokines, antigen presentation, as well as the absorption and lysis of pathogens. Beta (1,3)-glucan, a key component of the fungal cell wall, is known for its potent anti-inflammatory effect during infection. Pathogenicity can be decreased by greater exposure to beta (1,3)-glucan. Therefore, studies on beta (1,3)-glucan as an immunotherapy tactic are essential (Wagner et al. 2023).

Phytochemical screening is a preliminary test used for identifying the class of chemicals and summarizing secondary metabolites with biological activity. It serves as a starting point for identifying the class of chemical compounds contained in a plant. To determine the chemical compounds present in *Z. acanthopodium*, phytochemical screening was carried out using specific reagents. Secondary metabolite compounds are created to guard against diseases and insect problems, as well as adverse environmental factors, including temperature and climate. Additionally, these compounds are categorized according to chemical makeup, which includes triterpenoids, alkaloids, tannins, phenolics, saponins, flavonoids, and steroids (Hasibuan et al. 2021; Lubis et al. 2022).

A study conducted in India found that *Z. acanthopodium* extract demonstrated antifungal activity on *Candida krusei* and *C. albicans.* The petroleum ether extract proved to possess high antifungal activity compared to the rest of the solvent extracts. GC-MS analysis of petroleum ether extract identified 43 compounds. As compared to the standard Amphotericin-B, the crude extracts of *Z. acanthopodium* showed low antifungal action against two fungi, *C. krusei* and *C. albicans*. Compared to *C. albicans* (10 mm), *C. krusei* has a larger zone of inhibition (18 mm). The petroleum ether, compared to the other solvent extracts, showed strong antifungal activity (18 mm). MIC of the extracts against each of the five fungi was also calculated to ascertain the microbiological susceptibility. The petroleum ether extract had the lowest MIC (<0.9375 mg/mL) among all the extracts, against *C. krusei* (Kintamani et al. 2023).

Lipinski criteria are used to determine whether compounds and medications have similar qualities (drug-likeness). Compounds having superior pharmacological properties and those with high permeability and bioavailability can be screened using Lipinski criteria. When a compound has an octanol-water partition coefficient (log p)<5, a donor hydrogen bond value of <5, an acceptor hydrogen bond value of <10, and a molecular weight of <500 Da, it may be considered safe. A compound is deemed hazardous for use as a drug when it does not satisfy the Lipinski criteria (Fadlan et al. 2021).

The compound size is described by the molecular weight, which affects drug penetration capacity and ultimately the distribution process. Molecular weight determines the drug's capacity to diffuse through biological membranes passively. Molecules weighing more than 500 Da have low absorption rates due to their low capacity to cross the biological membrane. Among the two compounds found in this study, isodiosiprin and methylethyl-monoterpenoid, both satisfied the requirement of being less than 500 Da (Meylani et al. 2023). An important part of the Lipinski rule of five is the LogP parameter, which measures a compound's hydrophilicity and lipophilicity to assess oral bioavailability. The compounds methylethyl-monoterpenoid and isodiosiprin fit Lipinski requirements because the LogP values were less than 5 (Zhang et al. 2022).

The biological action of drug molecules is influenced by hydrogen bonding. According to Lipinski rule of 5, a compound should have no more than five hydrogen bond donors and no more than ten hydrogen bond acceptors. An excess of hydrogen bonding will harm the partition and permeability of the compound membrane. Polar groups created by hydrogen bonding potentially reduce a compound's affinity for the hydrophobic portion of the membrane, thereby decreasing the ability to cross the lipid bilayer membrane (Shaker et al. 2021). Table 7 demonstrates that methyl-monoterpenoid and isodiospyrene achieve these requirements. According to the Swiss-ADME site evaluation of Lipinski rule of five (Ro5) criteria, isodiosipyrine and methyl-monoterpenoid successfully passed the Ro5 requirements. The two phenolic compounds target the Beta Glucan domain on the *C. albicans* fungus's cell wall.

The molecular docking procedure also generates Gibbs free energy (ΔG) and inhibition constant values. The inhibition constant has a direct relationship with the bond free energy value. In general, the inhibition constant value decreases as the bond Gibbs free energy value (ΔG) decreases. The inhibition constant is the inhibitory concentration of ligand needed to prevent interaction with the protein. The stronger the interaction created, the lower the inhibition constant value. When six phenolic compounds were molecularly docked with EXO-B-(1.3)-Beta-glucanase *C.*

albicans protein on both active sides of the ligand, the inhibitory constant values were similar to the bond free energy value (ΔG). The values of the inhibition constant obtained were 1 and 150 μM.

The smallest inhibition constant value is found in 2,5-cyclohexadiene-1,4-dione, 3-hydroxy-2-methyl-5-(1-methylethyl) compound (52.37), suggesting that the bond formed in the interaction with Exo-B-(1.3)-glucanase receptor is better and more stable compared to other compounds. The hydrogen bonds in the test ligand have the same bond position as the native ligand. The 1-methyl-ethyl compound had the lowest inhibitory constant value among the docking test (Table 9). This compound has the lowest binding affinity value and the smallest inhibition constant value, suggesting that a better bond will form. The results also indicate the potential of the compound as a candidate for dengue antiviral medications in vitro or in vivo.

Isodiospyrin, a natural dimeric naphthoquinone, is a human DNA topoisomerase I (topoisomerase) inhibitor. The enzyme topoisomerase I is essential for transcription, DNA replication, and cell repair (Ting et al. 2003). The structural differences between the human and fungal topoisomerase I enzymes enable the creation of antifungal medications that specifically target the enzyme. Antifungal medications may have a fungicidal impact by interfering with cell growth and survival through topoisomerase I targeting. After serum induction in vitro, strains of *C. albicans* that experienced a deletion in the Topo I gene were unable to produce hyphae and form germ tubes. The Topo I gene is not necessary for the in vitro development of *C. albicans*, as demonstrated by the protein depletion under promoter repression. However, the morphological alterations caused by *C. albicans* growth in minimal media demonstrated that Topo I plays a significant role (Andrade-Pavón et al. 2024).

According to this study, isodiospyrin works against fungi by blocking the topoisomerase I enzyme. This mechanism is consistent with that of the active ingredient in echinocandin. A class of antifungals known as echinocandins has lipophilic side chains and cyclic non-ribosomal hexapeptides. Filamentous fungi produce these compounds, which have been used to create semisynthetic derivatives including caspofungin, micafungin, and anidulafungin, recognized as first-line antimycotics to treat invasive mycosis. The mode of action is by inhibiting 1,3-β-D-glucan synthase, which in turn disrupts the production of β-(1,3) d-glucan, a crucial polysaccharide found in cell walls (Nahar et al. 2024). This study demonstrates that isodiospyrin is a potential antifungal agent against *C. albicans*, with a nucleic acid-mediated mechanism of action. Further in vivo and in vitro studies are needed, along with investigations of other receptor proteins.

The antifungal efficacy in this study was evaluated just against *C. albicans* in vitro, leaving the spectrum of activity against other clinically significant fungal infections undetermined. The bioactive chemicals discovered via GC-MS and molecular docking were not purified nor individually evaluated, precluding the determination of each metabolite's unique contribution to the antifungal action. Even though in silico docking offered insightful information about possible binding interactions, in vivo models and clinical validation are still needed to confirm these findings. The study also only used a small number of bacterial isolates, which might not accurately reflect the variety of phyllosphere microbiota linked to *Z. acanthopodium.* Lastly, the current study did not examine how environmental factors, such as seasonal variations, geographic variance, and cultivation conditions, may affect metabolite production. Given the variation in phyllosphere bacteria's antifungal effectiveness across various environmental settings or geographic areas, it is critical to emphasize the significance of carrying out thorough research. It is true that variables like temperature, humidity, and the presence of different microbial communities can affect how successful these natural creatures are. We can gain a better understanding of how these microorganisms function in real-world situations by carrying out field research in a variety of environments and conditions. This study can assist in identifying particular strains that are robust and efficient, opening the door for customized uses in health and agriculture.

These bioactive molecules' distinct modes of action may offer particular benefits not found in conventional antifungals, enabling more focused therapies with fewer adverse effects. To maximize their therapeutic potential and minimize dangers, a comprehensive understanding of their interactions at the cellular and systemic levels is essential. Although docking methods have clear advantages, they are not dependable for estimating binding energies because of the simplistic scoring functions employed. Nevertheless, literature often presents comparisons among two or three complexes based on the predicted binding energies as a metric.

In conclusion, the phyllosphere bacteria of *Z. acanthopodium* demonstrated antifungal activity against *C. albicans* through both in vitro assays and in silico molecular docking analyses. Among the identified metabolites, isodiospyrin and 3-hydroxy-2-methyl-5-(1-methylethyl) showed strong binding affinities to the target protein, suggesting their potential as lead candidates for antifungal drug development. Molecular identification confirmed that the active isolates belonged to *Brevundimonas* sp. and *Pseudomonas* sp. Further studies are needed to separate specific antifungal compounds and retest the ability to inhibit *C. albicans*. Another recommendation for future studies is to optimize the production of potential antifungal compounds. *Z. acanthopodium* is quite abundant in Indonesia, especially in tropical areas, so it is necessary to explore it as an antifungal, so that it can become a candidate for antifungal drugs to solve the problem of resistance to antifungals.

ACKNOWLEDGEMENTS

This study was fully funded by a 2024 research grant from LPPM Universitas Bengkulu, Indonesia (Grant No. 2993/UN30.15/PT/2024).

REFERENCES

Adrian, Syahputra RA, Juwita NA, Astyka R, Lubis MF. 2023. Andaliman (*Zanthoxylum acanthopodium* DC.) a herbal medicine from North Sumatera, Indonesia: Phytochemical and pharmacological review. Heliyon 9 (5): e16159. https://doi.org/10.1016/j.heliyon.2023.e16159.

Andrade-Pavón D, Gómez-García O, Villa-Tanaca L. 2024. Review and current perspectives on DNA topoisomerase I and II enzymes of fungi as study models for the development of new antifungal drugs. J Fungi 10 (9): 629. https://doi.org/10.3390/jof10090629.

Atriwal T, Azeem K, Husain FM, Hussain A, Khan MN, Alajmi MF, Abid M. 2021. Mechanistic understanding of *Candida albicans* biofilm formation and approaches for its inhibition. Front Microbiol 12: 638609. https://doi.org/10.3389/fmicb.2021.638609.

Awidya IGB, Rizqoh D, Lestari N, Sipriyadi S, Sariyanti M. 2024. Strong potential of white cambodia (*Plumeria acuminata*) phyllosphere bacteria which inhibit *Candida albicans* growth. Bio Web Conf 127: 05002. https://doi.org/10.1051/bioconf/202412705002.

Baukova A, Bogun A, Sushkova S, Minkina T, Mandzhieva S, Alliluev I, Jatav HS, Kalinitchenko V, Rajput VD, Delegan Y. 2024. New insights into *Pseudomonas* spp.-produced antibiotics: Genetic regulation of biosynthesis and implementation in biotechnology. Antibiotics 13 (7): 597. https://doi.org/10.3390/antibiotics13070597.

Bras G, Satala D, Juszczak M, Kulig K, Wronowska E, Bednarek A, Zawrotniak M, Rapala-Kozik M, Karkowska-Kuleta J. 2024. Secreted aspartic proteinases: Key factors in *Candida* infections and host-pathogen interactions. Intl J Mol Sci 25 (9): 4775. https://doi.org/10.3390/ijms25094775.

Brion LP, Uko SE, Goldman DL. 2007. Risk of resistance associated with fluconazole prophylaxis: Systematic review. J Infect 54 (6): 521-529. https://doi.org/10.1016/j.jinf.2006.11.017.

Fadlan A, Warsito T, Sarmoko S. 2021. Pendekatan in silico dalam menyikapi potensi antikanker meciadanol. Jurnal Kimia Riset 6 (2): 163-171. https://doi.org/10.20473/jkr.v6i2.31071. [Indonesian]

Hasibuan PAZ, Harahap U, Sitorus P, Lubis MF, Satria D. 2021. In-silico analysis of vernonioside d and vernonioside e from *Vernonia amygdalina* Delile. leaves as inhibitor of Epidermal Growth Factor Receptor (EGFR) and mammalian Target of Rapamycin (mTOR). Rasayan J Chem 14 (3): 1539-1543. https://doi.org/10.31788/rjc.2021.1436092.

Huang J, Zaynab M, Sharif Y, Khan J, Al-Yahyai R, Sadder M, Ali M, Alarab SR, Li S. 2024. Tannins as antimicrobial agents: Understanding toxic effects on pathogens. Toxicon 247: 107812. https://doi.org/10.1016/j.toxicon.2024.107812.

Hutapea DB, Susilawati Y, Muhaimin M, Chaerunisaa AY. 2024. Potent bioactivity of andaliman (*Zanthoxylum acanthopodium* DC.). Pharmacia 71: 1-10. https://doi.org/10.3897/pharmacia.71.e117812.

Jawhara S. 2022. How gut bacterial dysbiosis can promote *Candida albicans* overgrowth during colonic inflammation. Microorganisms 10 (5): 1014. https://doi.org/10.3390/microorganisms10051014.

Johnston-Monje D, Raizada MN. 2021. Conservation and diversity of seed associated endophytes in *Zea* across boundaries of evolution, ethnography and ecology. PLoS One 6 (6): e20396. https://doi.org/10.1371/journal.pone.0020396.

Katiyar C, Gupta A, Kanjilal S, Katiyar S. 2012. Drug discovery from plant sources: An integrated approach. AYU 33 (1): 10-19. https://doi.org/10.4103/0974-8520.100295

Kintamani E, Batubara I, Kusmana C, Tiryana T, Mirmanto E, Asoka SF. 2023. Essential oil compounds of andaliman (*Zanthoxylum acanthopodium* DC.) fruit varieties and their utilization as skin anti-aging using molecular docking. Life 13 (3): 754. https://doi.org/10.3390/life13030754.

Logan A, Wolfe A, Williamson JC. 2022. Antifungal resistance and the role of new therapeutic agents. Curr Infect Dis Rep 24 (9): 105-116. https://doi.org/10.1007/s11908-022-00782-5.

Lubis MF, Kaban VE, Aritonang JO, Satria D, Mulina AA, Febriani H. 2022. Acute toxicity and antifungal activity of the ointment *Murraya koenigii* ethanol extract. Rasayan J Chem 15 (1): 256-261. https://doi.org/10.31788/rjc.2022.1516401.

Meylani V, Rizal Putra R, Miftahussurur M, Sukardiman S, Eko Hermanto F, Abdullah A. 2023. Molecular docking analysis of *Cinnamomum zeylanicum* phytochemicals against secreted aspartyl proteinase 4-6 of *Candida albicans* as anti-candidiasis oral. Results Chem 5: 100721. https://doi.org/10.1016/j.rechem.2022.100721.

Nahar D, Mohite P, Lonkar A, Chidrawar VR, Dodiya R, Uddin MJ, Singh S, Prajapati BG. 2024. An insight into new strategies and targets to combat antifungal resistance: A comprehensive review. Eur J Med Chem Rep 10: 100120. https://doi.org/10.1016/j.ejmcr.2023.100120.

Nikalje AP, Ramesh G. 2018. Liquid chromatography-mass spectrometry and its applications: A brief review. Arch Org Inorg Chem Sci 1 (1): 26-34. https://doi.org/10.32474/aoics.2018.01.000103.

Nurlaeni Y, Junaedi DI, Iskandar J. 2024. Botany, morphology, ecology, cultivation, traditional utilization and conservation of andaliman (*Zanthoxylum acanthopodium*) in North Sumatra, Indonesia. Nusantara Bioscience 16 (1): 68-80. https://doi.org/10.13057/nusbiosci/n160109.

Pelczar MJ, Chan ECS Jr. 2008. Dasar-Dasar Mikrobiologi. Universitas Indonesia Press, Jakarta. [Indonesian]

Pinzi L, Rastelli G. 2019. Molecular docking: Shifting paradigms in drug discovery. Intl J Mol Sci 20 (18): 4331. https://doi.org/10.3390/ijms20184331.

Pratama MRF, Poerwono H, Siswodihardjo S. 2021. Introducing a two-dimensional graph of docking score difference vs. similarity of ligand-receptor interactions. Indonesian J Biotechnol 26: 54-60. https://doi.org/10.22146/ijbiotech.62194.

Prieto-Martínez FD, Arciniega M, Medina-Franco JL. 2018. Molecular docking: Current advances and challenges. TIP Revista Especializada En Ciencias Químico-Biológicas 21: 65-87. https://doi.org/10.22201/fesz.23958723e.2018.0.143.

Rajamanickam K, Sudha SS, Francis M, Sowmya T, Rengaramanujam J, Sivalingam P, Prabakar K. 2013. Microalgae associated *Brevundimonas* sp. MSK 4 as the nano particle synthesizing unit to produce antimicrobial silver nanoparticles. Spectrochim Acta A Mol Biomol Spectrosc 113: 10-14. https://doi.org/10.1016/j.saa.2013.04.083.

Rizqoh D, Sipriyadi, Mas'ud N, Rahmawati ID, Sharon S, Suryani UH, Lestari N, Oktoviani, Wibowo RH. 2024a. Phyllosphere bacteria of andaliman (*Zanctoxylum acanthopodium* DC.) as potential antimicrobial compounds source against pathogenic bacteria. Front Health Inform 13 (3): 6399-6408.

Rizqoh D, Sipriyadi, Suryani UH, Putri CN, Agustin M, Taurustya H, Lestari N, Sariyanti M. 2024b. Exploring the antibacterial activity of endophytic bacteria from andaliman (*Zanthoxylum acanthopodium*) against *Bacillus subtilis*. Biodiversitas 25 (2): 700-707. https://doi.org/10.13057/biodiv/d250229.

Rizqoh D, Yolanda SD, Nugraheni E, Sipriyadi, Uliyandaria M, Wibowo RH, Oktoviani, Djatmiko EM, Putri AA. 2025. Antibacterial activity of phyllospheric bacteria isolated from *Rhizophora mucronata* against *Escherichia coli* and *Bacillus subtilis*. Biodiversitas 26 (1): 199-210. https://doi.org/10.13057/biodiv/d260121.

Shaker B, Ahmad S, Lee J, Jung C, Na D. 2021. In silico methods and tools for drug discovery. Comput Biol Med 137: 104851. https://doi.org/10.1016/j.compbiomed.2021.104851.

Soeka YS, Naiola E, Sulistyo J. 2007. Aktivitas antimikroba flavonoid - glikosida hasil sintesis secara transglikosilasi enzimatik. Berita Biologi 8: 455-464. [Indonesian]

Steven B, Huntley RB, Zeng Q. 2018. The influence of flower anatomy and apple cultivar on the apple flower phytobiome. Phytobiomes J 2 (3): 171-179. https://doi.org/10.1094/pbiomes-03-18-0015-r.

Ting C-Y, Hsu C-T, Hsu H-T, Su J-S, Chen T-Y, Tarn W-Y, Kuo Y-H, Whang-Peng J, Liu LF, Hwang J. 2003. Isodiospyrin as a novel human DNA topoisomerase I inhibitor. Biochem Pharmacol 66 (10): 1981-1991. https://doi.org/10.1016/j.bcp.2003.07.003.

Vetvicka V, Teplyakova TV, Shintyapina AB, Korolenko TA. 2021. Effects of medicinal fungi-derived β-glucan on tumor progression. J Fungi 7 (4): 250. https://doi.org/10.3390/jof7040250.

Wagner AS, Lumsdaine SW, Mangrum MM, Reynolds TB. 2023. Caspofungin-induced β(1,3)-glucan exposure in *Candida albicans* is driven by increased chitin levels. mBio 14 (4): e0007423. https://doi.org/10.1128/mbio.00074-23.

Wiederhold NP. 2017. Antifungal resistance: Current trends and future strategies to combat. Infect Drug Resist 10: 249-259. https://doi.org/10.2147/idr.s124918.

Yu Z, Wu X, He J. 2022. Study on the antifungal activity and mechanism of tea saponin from *Camellia oleifera* cake. Eur Food Res Technol 248: 783-795. https://doi.org/10.1007/s00217-021-03929-1.

Zhang B, Li H, Yu K, Jin Z. 2022. Molecular docking-based computational platform for high-throughput virtual screening. CCF Trans High Perform Comput 4 (1): 63-74. https://doi.org/10.1007/s42514-021-00086-5.